International Journal of GEOMATE, March, 2017, Vol. 12, Issue 31, pp. 23-29
Geotec., Const. Mat. & Env., ISSN:2186-2990, Japan, DOI: http://dx.doi.org/10.21660/2017.31.6513

DEM MODELLING OF GEOCELL-STABILISED SUB-BALLAST UNDER CYCLIC LOADING

* Ngoc Trung Ngo[1], Cholachat Rujikiatkamjorn[1] and Buddhima Indraratna[1]

[1]Centre for Geomechanics and Railway Engineering, Faculty of Engineering and Information Sciences, University of Wollongong, Wollongong, NSW 2522, Australia.

*Corresponding Author, Received: 28 April 2016, Revised: 08 June 2016, Accepted: 29 Nov. 2016

ABSTRACT: Upon repeated train loading, sub-ballast aggregates, placed underneath a ballast layer in rail track, become degraded and fouled by the progressive accumulation of external fine particles such as mud-pumping of soft subgrade, seriously decreasing the shear strength and drainage capacity of the track. This paper presents a study of the load-deformation response of geocell-reinforced sub-ballast under cyclic loads using laboratory tests and discrete element method (DEM). A series of large-scale cubical triaxial tests with and without geocell inclusions are conducted in the laboratory and simulated in DEM to investigate the beneficial effect of the geocells in decreasing the lateral and vertical deformations of railway subballast. Irregularly-shaped particles of sub-ballast are modelled by connecting and bonding of many circular balls together at appropriate sizes and positions. The geogcell was simulated by bonding many small spheres together to build a desired geometry and structure. The load-deformation behaviour of the geocell-stabilised sub-ballast specimen at varied load cycles predicted from the DEM modelling agrees well with those measured experimentally, showing that the proposed DEM model in this study is able to capture the deformation behaviour of the sub-ballast stabilised by the geocell. Additionally, the DEM modelling also provides insight into the distribution of contact forces, average contact normal and shear forces, which cannot be determined experimentally. These observations clearly prove the reinforcement effect of the geocell in eliminating the deformation of sub-ballast from a micromechanical perspective.

Keywords: Geocell, Discrete Element Method, Subballast, Cyclic Loading

1. INTRODUCTION

In view of rapid urbanization, the demand for suitable ground improvement solutions is imperative, in order to construct roads and rail infrastructure over soft soils. This results in intensified stress on railway industry to find innovative approaches to maintain track stability and reduce maintenance cost. The use of planar geosynthetics (e.g. geogrids, geotextiles or geocomposites) has proven as a promising technique to strengthen the shear strength of granular media placed over weak and soft deposits [1]-[3]. Loss of track geometry that is often associated with excessive differential settlements due to localized failure of formation (capping and subgrade), often leads to decreased stability and reduced track longevity [4]. In this regard, planar geosynthetics has been effectively utilised to reduce excessive settlements and lateral displacements of ballasted rail tracks [5]. In recent times, three-dimensional cellular reinforcement, also known as geocell mattress, has been used for different applications. The improved performance of geocell-stabilised soil has been attributed to enhanced apparent cohesion between the infilled soil and the geocell [6]. Nevertheless, recent studies have proven that the additional confinement mobilised during cyclic loading, helps to enhance confinement and minimize lateral spreading of the aggregates, hence maintain stability of the infill granular material [7]. In order to determine the effects of geocells, different types of geocells have been widely used. Also, the effects of aperture size and shape and opening area have been investigated by employing large-scale direct shear box and assessing the shear strength of unreinforced and reinforced soil [6], [7].

There has been limited research carried out to study the effect of geocell mattress on railway substructure, where the benefits of geocell under cyclic loading have not been investigated in details either in laboratory or numerical modelling [8]. The development of computational models that have been validated appropriately by either laboratory or field measurements is thereby inevitable to study the enhanced performance of geocell-reinforced sub-ballast and to derive proper design guidelines for ballasted track, considering the confinement effect provided by geocells [9]. An extensive attempt has been made in this study to conduct large-scale cubical triaxial tests of geocell-reinforced sub-ballast and to develop a discrete element model (DEM) simulating the composite system, capturing the additional confinement provided by the geocell to the infilled

sub-ballast.

The discrete element method (DEM) introduced by [10] has been widely used to study stress-strain behaviour of granular materials [11]-[15]. It is noted that there have been limited research on the use of DEM to simulate rail sub-ballast under cyclic loads with high numbers of load cycles. Lu and McDowell [16] carried out DEM analysis to model fresh ballast under 100 load cycles and showed that the DEM can capture the stress-strain behaviour of ballast that are comparable with 500,000 cycles in laboratory. Ngo et al. [12] conducted DEM analysis to investigate the performance of geogrid stabilised ballast fouled with coal, and presented that the interlock of the aggregates with geogrid was the main causes for improved performance of the composite assembly. It would also be noted that there has been limited past DEM studies on the behavior of geocell-reinforced ballast under a high numbers of load cycles and varied frequencies. Lobo-Guerrero and Vallejo [17] conducted DEM simulations of model tests for the ballast layer subjected to a total of 425 load cycles. Results indicated that stone-blowing was very effective while the use of geosynthetics was found to be less beneficial. This is because the DEM used circular bonded particles, and the simulations were limited to only a few hundred load cycles.

In this study, experimental tests were carried out and the discrete element method (DEM) was used to model geocell-reinforced sub-ballast subjected to cyclic train loading, capturing the deformation and corresponding micro-mechanical characteristics of this composite assembly. The current DEM analysis was able to include irregular shapes of particles to better represent the role of angularity, whereby up to 10,000 load cycles could be performed with different frequencies, and in this respect the current study is an original attempt to capture the more realistic behaviour of the plastic deformation of geocell-reinforced sub-ballast over a much longer cyclic loading duration.

2. EXPERIMENTAL STUDY

A large-scale cubical triaxial apparatus (800 mm long, 600 mm wide and 600 mm high) was designed and built at the University of Wollongong (Fig.1), and it was used to investigate the stress-strain behaviour of the unreinforced and geocell-reinforced subballast subjected to cyclic loading [6], [9]. The area of the test specimen in the cubical triaxial chamber was selected based on Australian standard gauge for heavy haul track with an approximate plan area of 800mm × 600mm, and 600 mm height. The sub-ballast

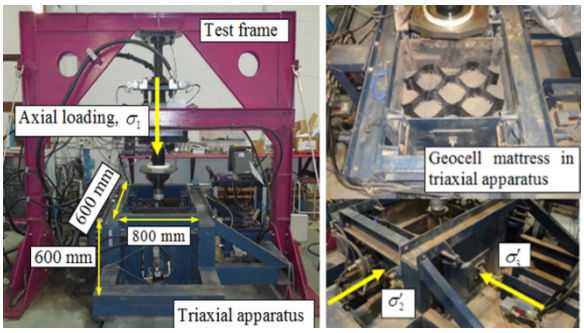

Fig. 1 Cubical triaxial apparatus used in this study.

material had a total depth of 450 mm, of which the upper 150mm was stabilised by geocell, as shown in Fig. 1. The material for sub-ballast used in this study was a locally available crushed basalt, collected from a quarry near Wollongong (NSW, Australia). The particle size distribution adopted for the sub-ballast was within the Australian rail industry specified range (D_{50} = 3.3 mm, D_{max} = 19 mm, D_{min} = 0.075 mm, C_u = 16.3, C_c = 1.3, unit weight, γ = 18.5 kN/m3). A geocell mattress made from polyethylene materials, that was connected at the joints to create a three-dimensional cellular form (i.e. depth = 150 mm, ultimate tensile strength = 9.5 kN/m, thickness = 1.3 mm, density = 950 kg/m3) was used. A predetermined mass of sub-ballast was placed inside the cubical box in several layers and compacted using a vibratory hammer to achieve a relative density (*DR*) of about 77%, which is representative of the density of sub-ballast in the field [6]. A geocell mattress was placed onto the surface of the sub-ballast. All specimens were prepared until the layer of sub-ballast reached a final height of 450 mm.

The experiments were conducted under plane strain condition, where any lateral movement in the longitudinal direction (parallel to the track) was restricted (ε_2=0). The walls were allowed to move laterally in the direction parallel to the sleeper (or tie) ($\varepsilon_3 \neq 0$), to simulate a long straight section of track. Laboratory tests were carried out in a stress-controlled manner, where the magnitudes of the cyclic stresses were determined based on 30 tons/axle load. To investigate the influences of confining pressures on the load-deformation of sub-ballast, cyclic tests were conducted at varying confining pressures of, σ_3= 5, 10, 15, 20, 30 kPa and frequencies of f=10, 20, 30 Hz. Initially, a monotonic strain-controlled load was applied to the specimen at a rate of 1 mm/min until a mean level of cyclic deviator stress was

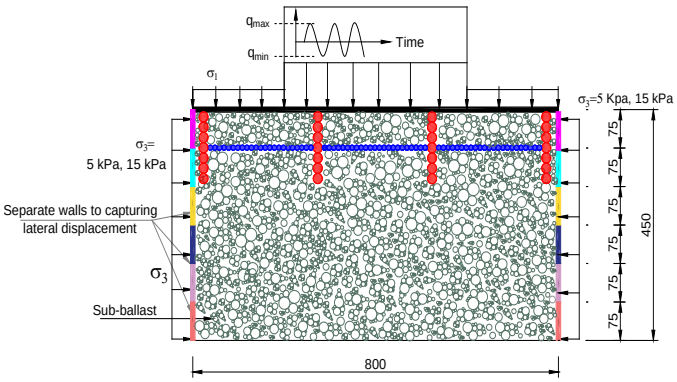

Fig. 2 Schematic DEM model used to calibrate sub-ballast micromechanical parameters (dimensions in mm).

attained. Subsequently, a stress controlled cyclic loading using a positive full-sine waveform was applied to the specimens where a maximum and minimum stress of qmax = 166 kPa and qmin = 41 kPa was used to simulate subballast under a heavy haul freight network operating in NSW [7],[18], [19], [20].

Laboratory test results showed that the confining pressure (σ_3) and frequency (f) induce a significant impact on the load-deformation behaviour of the sub-ballast under cyclic loading. The experimental data confirmed that under cyclic loading, geocell mattress can offer additional confinement ($\Delta\sigma_3$) to the infill material (i.e. other than the confining pressure available from sleepers and shoulder ballast), and help to decrease the axial and lateral deformations [9]. Also it is noted that due to cyclic loading, the magnitude of would be increase as the number of load cycle increases and when the densely compacted infill material dilates and thereby increases the magnitude of hoop stress. A summary of the key aspects of experimental outcomes can be briefly summarised as: (i) the mobilised hoop stress of the geocell pockets is generated as a result of the dilation of the infilled soil during shearing; and (ii) the magnitude of hoop stress varies with the geocell modulus [6], [7],],[18].

3. DISCRETE ELEMENT MODELLING

In DEM, the force-displacement law derives the contact force acting on two particles (e.g. *A* and *B*) in contact with the relative displacement between them. The force vector $\vec{\boldsymbol{F}}$ is described into normal ($\vec{\boldsymbol{F}}_{\boldsymbol{N}}$) and shear component ($\vec{\boldsymbol{F}}_{\boldsymbol{T}}$) with respect to the contact plane:

$$\vec{\boldsymbol{F}}_{\boldsymbol{N}} = \boldsymbol{K}_{\boldsymbol{N}} \cdot \boldsymbol{U}^{\boldsymbol{n}} \quad (1)$$

$$\boldsymbol{\delta}\vec{\boldsymbol{F}}_{\boldsymbol{T}} = -\boldsymbol{K}_{\boldsymbol{T}} \cdot \boldsymbol{\delta U}^{\boldsymbol{s}} \quad (2)$$

where, $\boldsymbol{K}_{\boldsymbol{N}}$ and $\boldsymbol{K}_{\boldsymbol{T}}$ are the normal and shear stiffnesses at the contact; $\boldsymbol{\delta U}^{\boldsymbol{s}}$ is the incremental shear displacement, and $\boldsymbol{\delta}\vec{\boldsymbol{F}}_{\boldsymbol{T}}$ is the incremental shear force.

The normal contact stiffness for the linear contact model used in this study was computed as:

$$\boldsymbol{K}_{\boldsymbol{N}} = \frac{\boldsymbol{k}_{\boldsymbol{n}}^{[A]}\boldsymbol{k}_{\boldsymbol{n}}^{[B]}}{\boldsymbol{k}_{\boldsymbol{n}}^{[A]}+\boldsymbol{k}_{\boldsymbol{n}}^{[B]}} \quad (3)$$

and the contact shear stiffness is given by:

$$\boldsymbol{K}_{\boldsymbol{T}} = \frac{\boldsymbol{k}_{\boldsymbol{s}}^{[A]}\boldsymbol{k}_{\boldsymbol{s}}^{[B]}}{\boldsymbol{k}_{\boldsymbol{s}}^{[A]}+\boldsymbol{k}_{\boldsymbol{s}}^{[B]}} \quad (4)$$

where, $\boldsymbol{k}_{\boldsymbol{n}}^{[A]}$, $\boldsymbol{k}_{\boldsymbol{n}}^{[B]}$, $\boldsymbol{k}_{\boldsymbol{s}}^{[A]}$, $\boldsymbol{k}_{\boldsymbol{s}}^{[B]}$ are the normal stiffness and shear stiffness of particle *A* and *B*, respectively.

The new shear contact force is determined by summing the old shear force existing at the start of the time-step with the shear elastic force increment

$$\vec{\boldsymbol{F}}_{\boldsymbol{T}} \leftarrow \vec{\boldsymbol{F}}_{\boldsymbol{T}} + \boldsymbol{\delta}\vec{\boldsymbol{F}}_{\boldsymbol{T}} \leq \boldsymbol{\mu}\,\vec{\boldsymbol{F}}_{\boldsymbol{N}} \quad (5)$$

where, $\boldsymbol{\mu}$ is the coefficient of friction.

3.1 DEM Modelling of Cubical Triaxial Test

A two-dimension DEM analysis was conducted to study the interaction between geocell and sub-ballast by simulating the cubical triaxial tests that were carried out in the laboratory, as illustrated in Fig. 2. The angular-shaped grains of sub-ballast were simulated by connecting a number of circular-shaped particles together, mimicking the actual sub-ballast shape and angularity [21], [22], [23], [24]. A total of 26,567 particles, with sizes ranging from 0.5 to 19 mm, were generated to simulate actual sub-ballast

Table 1 Micromechanical parameters used to simulate sub-ballast and geocell in DEM

Items	Sub-ballast	Geocell
Particle density (kN/m$^{3)}$	15.5	18.5
Coefficient of friction	0.72	0.45
Contact normal stiffness (N/m)	2.56×10^8	6.51×10^6
Contact shear stiffness, k_s (N/m)	2.56×10^8	6.51×10^6
Parameter of contact bond normal strength, $\boldsymbol{\phi_n}$(kN)	5.36×10^6	43.2
Parameter of contact bond shear strength, $\boldsymbol{\phi_s}$ (kN)	8.53×10^6	43.2
Parallel bond radius multiplier, r_p	0.5	0.5
Parallel bond normal stiffness, k_{np} (kPa/m)	4.86×10^7	4.86×10^7
Parallel bond shear stiffness, k_{sp} (kPa/m)	4.86×10^7	4.86×10^7
Parallel bond normal		

strength, σ_{np} (MPa)	352	352
Parallel bond shear strength, σ_{sp} (MPa)	352	352

gradation with a representative field unit weight approximately of 18.5 kN/m^3. Particles were generated in the assembly at random orientations to resemble experimental conditions. Micromechanical parameters to model sub-ballast (e.g. shear and normal contact stiffness, friction coefficient) selected in the current DEM analysis were determined based on the process of calibration of DEM results with the experimental data, as presented in Table 1. The geocell pocket structure was modeled by bonding balls of 20 mm-diameter and 10 mm-diameter to form vertical and horizontal panels, respectively. This simplified geocell structure was presumed to be adequate to provide the confinement effect for the sub-ballast packed inside the cellular pockets. Micromechanical parameters (Table 1) to model the geocell were determined based on a series of simulated tensile tests and compared the tensile force-strain response with data measured experimentally.

4. RESULTS AND DISCUSSION

The DEM model for the plane strain cubical triaxial tests was used to simulate geocell-reinforced sub-ballast subjected to a confining pressure of σ_3=10 kPa and cyclic frequencies of 10, 20, and 30 Hz, similar to the loading conditions conducted in the laboratory. DEM simulations to model the sub-ballast with and without geocell inclusions were simulated up to 10,000 load cycles, where most of the sub-ballast deformation had taken place as observed in the laboratory. During loading, vertical positions and lateral movements of the sub-ballast assemblies were recorded to determine the associated settlements and lateral displacements at corresponding load cycles.

4.1 Settlements of Sub-ballast with and without Geocell

The average accumulated settlement at different load cycles obtained from DEM simulations compared to the experimental results are presented in Fig. 3. Results obtained from DEM analysis matched reasonably well with the experimental data at any given frequency and confining pressure. The predicted and measured data indicated that the settlement increased with an increase in frequency.

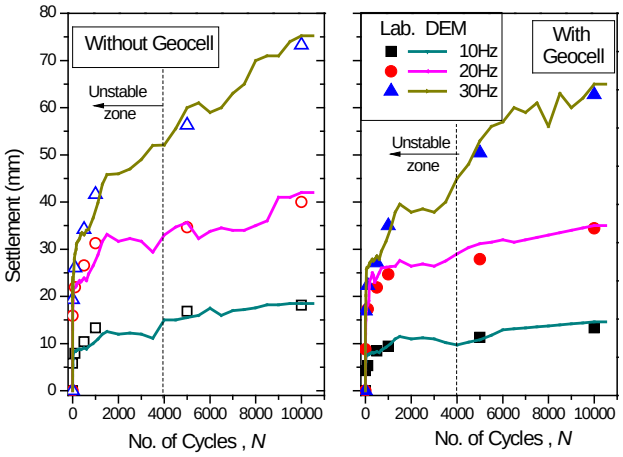

Fig. 3 Settlement versus load cycles measured experimentally and predicted in DEM (modified after Ngo *et al*. [9]).

Geocell-reinforced sub-ballast exhibited less settlement than that of the unreinforced assembly. Undoubtedly, this is a result of additional confining pressure provided by the geocell would decrease the deformation of sub-ballast. When the sub-ballast aggregates were compacted over a geocell, they were projected through the geocell pockets and generated a strong mechanical (i.e. acting as a non-displacement boundary) which results in reduced settlement. Additionally, the settlement accelerated significantly during the first few thousand cycles due to initial particle compression and rearrangement, and then the settlement increased at a diminished rate in the subsequent load cycles and approached an approximately constant rate at very high load cycle.

4.2 Contact Force Distributions of Geocell-reinforced Sub-ballast

Contact forces in a sub-ballast assembly are transferred through an inter-connected network of force chains via contact points. Fig. 4a presents contact force distributions of an unreinforced sub-ballast specimen subjected to the cyclic load at a given frequency of 20 Hz at a settlement (S) of 5 mm, while Figs. 4b-d show the contact force distributions of geocell-reinforced sub-ballast at settlements of S=5 mm, 15 mm, and 20 mm, respectively. It is noted that the contact forces among particles are plotted as lines on the same scale, whose thickness is proportional to its magnitude, and for clarity, only those contacts with a magnitude exceeding the average force of the whole assembly are presented. They clearly show that the total number of contact forces and maximum contact forces increase as settlement

increases, and this can be attributed to the assembly was compacted and compressed to sustain the external load. For instance, with reinforced sub-ballast, the number of contacts is 60,252 for the settlement of 5 mm, and it increases to 78,252 and 83,521 contacts for settlements of *S*=15 and 20 mm, respectively.

Maximum contact forces also increases with an increase of settlements, and these are 745 N, 857 N and 946 N for the settlements of *S*=5, 15 and 20 mm, respectively. Compared to the unreinforced sub-ballast (Fig. 3a), the reinforced assemblies created more contacts within the geocell regions, and this could be associate d with the confinement the geocell provided to the infilled sub-ballast. It can also be seen that the tensile forces (in red colour) in geocells are mobilised with an increased in settlement.

4.3 Variations of Contact Normal and Shear Forces

Fig. 5 presents the variations of contact normal and shear forces with depth for reinforced and unreinforced sub-ballast (at N=10,000 cycles). Compared to the unreinforced cases (Figs. 5c, 5d), geocell-reinforced sub-ballast assemblies exhibit a significant increase in the contact force within the geocell zone, but underneath the geocell the average normal and shear contact forces decrease with depth and approach almost constant values near the bottom of the assembly. Undoubtedly the inclusion of geocell decreases the shear and normal contact force in sub-ballast below the geocell. It is worth mentioning that the micro-mechanics of the geocell-reinforced sub-ballast conducted in this study was limited to the distribution of contact force chains and the average contact normal and shear force distributions. However, the comparison of the experimental observations with the 2D plane strain DEM analysis proves that to the current analysis was able to capture the load-deformation behaviour of geocell-stabilised sub-ballast in spite of these limitations. Generally, the authors have made a few simplifications to keep the micro-mechanical analysis fairly simples, as the requirements of brevity of this paper would not allow the reporting of more detailed DEM analyses that could capture other micro-mechanical aspects such as the evolution of fabric anisotropy and complex detailing of changing angularity with the high number of loading cycles.

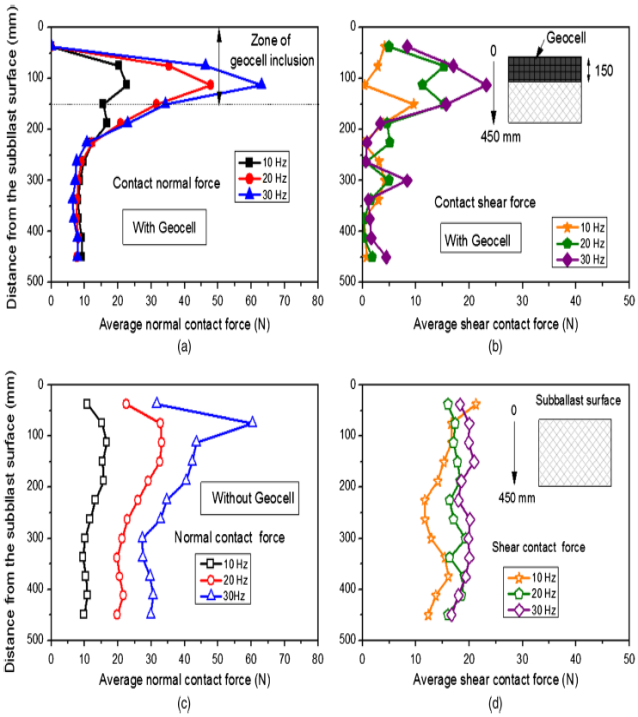

Fig. 5 Distributions of contact normal and shear forces: (a) and (b) - with geocell inclusion; (c) and (d) - without geocell.

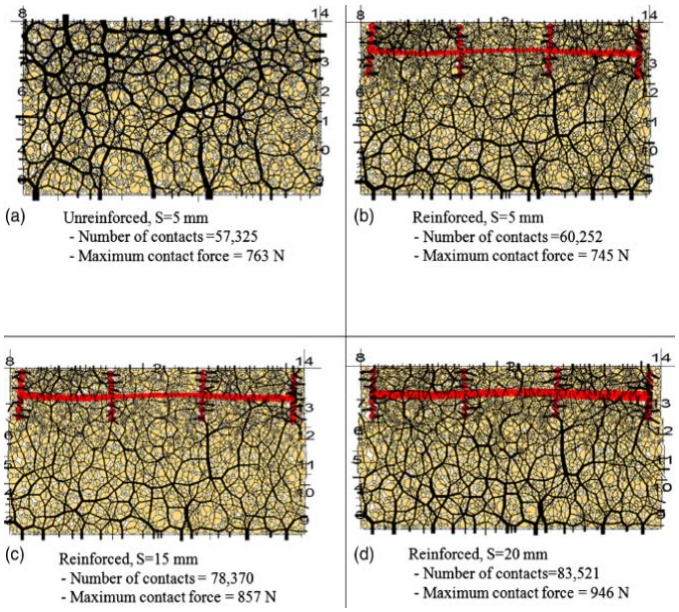

Fig. 4 Distribution of contact forces for unreinforced and reinforced subballast at varied settlements (modified after Ngo *et al*. [9])

5. CONCLUSION

A series of large-scale cubical triaxial tests were carried out on sub-ballast with and without geocell inclusion, and then the results were used to calibrate and compare with the DEM analysis. Irregular particles of sub-ballast were simulated by clumping several circular balls together to represent appropriate angularity. Geocell was modelled in 2D plane strain DEM model by bonding small balls together to form the cellular

pockets with contact and parallel bonds. A set of micromechanical parameters to simulate sub-ballast and geocell were determined by comparing with laboratory test data. Once these parameters were properly validated, they were used to simulate the cubical triaxial tests for testing sub-ballast subjected to cyclic loading at frequencies of 10 Hz, 20 Hz and 30 Hz. Experimental data of settlements and lateral displacements were comparable with those obtained from DEM simulations at a given frequency and confining pressure, indicating that the DEM model proposed in this study could simulate the load-deformation behaviour of a geocell-reinforced sub-ballast assembly. As the frequency increased, the settlement and lateral deformations of sub-ballast increased, but unlike the unreinforced sample, the geocell-reinforced sub-ballast exhibited remarkably less deformation. This was undoubtedly attributed to the confinement provided by geocell that prevented sub-ballast aggregates from free movement that would otherwise occur.

Contact force distributions of geocell-reinforced sub-ballast were presented. DEM results showed that the total number of contact force distributions and the maximum contact force increased with increased deformation. The contact normal and shear forces developed among sub-ballast particles at varied depths were also captured. The magnitudes of these forces within the geocell zone were considerably higher than at other locations. Underneath the geocell, these contact forces continuously decreased with depth and approached almost constant values near the bottom of the granular assembly.

6. ACKNOWLEDGEMENTS

The Authors would like to acknowledge the Rail Manufacturing CRC, Australasian Centre for Rail Innovation (ACRI) Limited, and Tyre Stewardship Australia Limited for providing the financial support needed to undertake this research (Project R2.5.1). The Authors thank to Dr Mahdi Biabani and laboratory assistance from technicians, Alan Grant and Ian Bridge during the laboratory tests. The Authors would also appreciate the kind permission from the Journal of Geotechnical and Geoenvironmental Engineering - ASCE for reproducing selected content in this paper.

7. REFERENCES

[1] Bergado, D. T., Chai, J. C., Abiera, H. O., Alfaro, M. C., and Balasubramaniam, A. S. (1993). "Interaction between cohesive-frictional soil and various grid reinforcements". Geotext Geomembranes. 12(4): 327-349.

[2] Indraratna, B., Ngo, N.T., and Rujikiatkamjorn, C. (2011b). "Behaviour of geogrid-reinforced ballast under various levels of fouling". Geotext and Geomembranes. 29(3): 313-322.

[3] Rujikiatkamjorn, C., Indraratna, B., Ngo, N.T. and Coop, M., 2012. “A laboratory study of railway ballast behaviour under various fouling degree”. Proceedings of the 5th Asian Regional Conference on Geosynthetics (GA2012), D. T. Bergado (Eds.), pp: 507-514

[4] Selig, E. T. , and Waters, J. M. (1994). “Track geotechnology and substructure management”, Thomas Telford, London.

[5] Indraratna, B., Ngo, N.T. , and Rujikiatkamjorn, C. (2013). "Studying the deformation of coal fouled ballast stabilised with geogrid under cyclic load". J. Geotech. Geoenviron. Eng., 139(8): 1275–1289.

[6] Biabani, M. M., Indraratna, B., and Ngo, N. T. (2016). “Modelling of geocell-reinforced subballast subjected to cyclic loading”. Geotext Geomembranes. 44(4), pp: 489-503.

[7] Biabani, M. M., Ngo, N. T., and Indraratna, B. (2016). “Performance evaluation of railway subballast stabilised with geocell based on pull-out testing”. Geotext Geomembranes.44(4): 579–591.

[8] Leshchinsky, B. and Ling, H., 2013a. Effects of geocell confinement on strength and deformation behavior of gravel. J. Geotech. Geoenviron. Eng., 139(2), 340-352.

[9] Ngo, N.T., Indraratna, B., Rujikiatkamjorn, C., and Biabani, M. (2016). "Experimental and discrete element modeling of geocell-stabilized subballast subjected to cyclic Loading”, J. Geotech. Geoenviron. Eng.,42(4):04015100.

[10] Cundall, P. A. , and Strack, O. D. L. (1979). "A discrete numerical model for granular assemblies". Géotechnique. 29(1): 47-65.

[11] Lim, W. L. , and McDowell, G. R. (2005). "Discrete element modelling of railway ballast". Granular Matter. 7(1): 19-29.

[12] Ngo, N.T., Indraratna, B., and Rujikiatkamjorn, C. (2014). "DEM simulation of the behaviour of geogrid stabilised ballast fouled with coal". Computers and Geotechnics. 55: 224-231.

[13] Indraratna, B., Ngo, N.T., Rujikiatkamjorn, C. , and Vinod, J. (2014). "Behaviour of fresh and fouled railway ballast subjected to direct shear testing - a discrete element simulation". Int. J. Geomech. , 14(1): 34-44.

[14] Indraratna, B., Ngo, N.T., Rujikiatkamjorn, C. & Sloan, S. W. (2015). Coupled discrete element–finite difference method for analysing the load-deformation behaviour of a single stone column in soft soil. Computers and Geotechnics, 63 267-278.

[15] Ngo, N. T., Indraratna, B. & Rujikiatkamjorn, C. (2015). A study of the behaviour of fresh and coal fouled ballast reinforced by geogrid using the discrete element method. In K. Soga, K. Kumar, G. Biscontin & M. Kuo (Eds.), Geomechanics from Micro to Macro (pp. 559-563). United Kingdom: Taylor & Francis. 2014.

[16] Lu, M. , and McDowell, G. R. (2010). "Discrete element modelling of railway ballast under monotonic and cyclic triaxial loading". Geotechnique. 60(6): 459-467.

[17] Lobo-Guerrero, S. , and Vallejo, L. E. (2010). "Crushing of particles under simulated static and centrifuge forces". GeoFlorida 2010: Advances in Analysis, Modeling & Design (Geotechnical Special Publication, 199), ASCE. 550-559.

[18] Indraratna, B., Biabani, M.M., Nimbalkar, S., 2015. Behaviour of geocell reinforced subballast subjected to cyclic loading in plane strain condition. J. Geotech. Geoenviron. Eng. 141 (1), 04014081-1-16.

[19] Ngo, N.T, and Tung, T. (2016). “Coupled discrete-continuum method for studying load-deformation of a stone column reinforces rail track embankments”. Procedia Engineering, 142 138-144.

[20] Ngo, N.T, Indraratna, B., and Rujikiatkamjorn, C. (2016). "Micromechanics-Based Investigation of Fouled Ballast Using Large-Scale Triaxial Tests and Discrete Element Modeling." J. Geotech. Geoenviron. Eng., 10.1061/(ASCE)GT.1943-5606.0001587 , 04016089.

[21] Ngo, N.T., Indraratna, B. and Rujikiatkamjorn, C. (2016)"Modelling geogrid-reinforced railway ballast using the discrete element method." Transportation Geotechnics, 8(2016), pp: 86-102.

[22] Ngo, N.T. and Indraratna, B. (2016). "Improved Performance of Rail Track Substructure Using Synthetic Inclusions: Experimental and Numerical Investigations." Int. J. of Geosynth. and Ground Eng., 2(3), pp: 1-16.

[23] Yang, Y., Li, N., Yin, P. and Cheng, Y.M., 2013. “Flow pattern for multi-size silos”, Int. J. of GEOMATE, Dec, 2013, Vol. 5, No. 2 (Sl. No. 10), pp. 712-716.

[24] Kumara, J., Hayano, K., Shigekuni, Y. and Sasaki, K. (2013). Physical and mechanical properties of sand-gravel mixtures evaluated from DEM simulation and laboratory triaxial test. Int. J. of GEOMATE, 4(2), pp.546-551.